Historical and future land use and land cover changes in the Fincha watershed, Ethiopia

Motuma Shiferaw Regasa

Polish Academy of Sciences Institute of Geophysics: Polska Akademia Nauk Instytut Geofizyki

Michael Nones (mnones@igf.edu.pl)

Polish Academy of Sciences Institute of Geophysics: Polska Akademia Nauk Instytut Geofizyki https://orcid.org/0000-0003-4395-2637

Research Article

Keywords: Ethiopia, Fincha Basin, Land use Land Cover, Land Change Modeler, Multi-Layer Markov Chain

Posted Date: October 22nd, 2021

DOI: https://doi.org/10.21203/rs.3.rs-978807/v1

Abstract

The increasing human pressure on African regions is recognizable from land use land cover (LULC) changes maps, as derived from satellite imagery. Using the Ethiopian Fincha watershed as a case study, the present work focuses on i) identifying historical LULC change in the period 1989-2019; ii) estimating LULC in the next thirty years, combining Geographical Information Systems (GIS) with Land Change Modelling (LCM). Landsat5/8 images were combined with field evidence to map LULC in three reference years (1989, 2004, 2019), while the Multi-Layer Markov Chain (MPL-MC) model of LCM was applied to forecast LULC in 2030, 2040 and 2050. The watershed was classified into six classes: waterbody, grass/swamp, built-up, agriculture; forest and shrub. The results have shown that, in the past 30 years, the Fincha watershed experienced a reduction of forest and shrubs due to ever-increasing agricultural activities, and such a trend is also expected in the future. In addition, the decrease in areas covered by natural forests can drive to an increase in soil erosion, fostering the siltation in the water reservoirs located in the basin. The study pointed out the urgency of taking actions in the basin to counteract such changes, which can eventually drive to a less sustainable environment.

1. Introduction

Land use is defined as how the land is utilized by human beings and their habitats, usually with an accent on a practical role of land for economic activities, whereas land cover is a physical characteristic of the Earth's surface or attributes of a part of the Earth's land surface and immediate subsurface, including biota, soil, topography, surface and groundwater, and human structures (Alan et al. 2020; Leta et al. 2021a; Regasa et al. 2021; Tadese et al. 2021). As it strictly connected with representing the hydrological cycle (Dwivedi et al. 2005), land use and land cover (LULC) change has been one of the most widely used methods to comprehend past land uses, types of changes estimated, the forces behind such changes and the perceptible transformations of the Earth's surface (Alam et al. 2020). LULC changes could involve critical issues such as biodiversity degradation and negative impact on human life (Kenea et al. 2021; Khan et al. 2021). The study of LULC change has attracted growing interest in recent years, as it is a complex issue that involves physical, environmental, and socioeconomic facts. According to Lambin et al. (2000), the modelling of land cover processes can answer questions like i) which are the main environmental and cultural variables that contribute most to the observed changes, and why? ii) within a geographical region, which location can be affected by land cover changes, where and at what rate do land cover change and when?

Prediction using time serious data is important for the future management plan of LULC, and it is frequently employed for a diverse appropriateness measure as a proxy of human influence on land change processes (Han et al., 2015; Tadese et al. 2021). Analysis of the historical trends of LULC is paramount in modelling future LULC, as past information are generally representing a good proxy of human influence on land processes (Han et al., 2015; Rahman et al., 2017). To adequately predict future scenarios, models should be calibrated and validated, and various techniques are available in the literature. Geometric rectifying, supervised and unsupervised classification methods, post-classification method, GIS spatial analysis, Markov chain analysis, ERDAS imagine model and Land Change Modeler (LCM) were used to analyze historical LULC change and predict future changes (Fan et al. 2008).

The Land Change Modeler is a model used to evaluate the changing trend from one land use category to another and has been found to provide high spatial and temporal resolution with a reduced computational effort (Etemadi et al. 2018; Leta et al. 2021b). The integrated CA–Markov model is a robust technique in terms of quantity estimation as well as spatial and temporal dynamic modelling of LULC, because remote sensing data and GIS can be proficiently incorporated. Integrated CA–Markov model can translate the results of the Markov chain model to spatially explicit results (Al-sharif et al. 2014). The Markov model has been widely adopted in ecological studies, and its applicability in LULC change modelling is promising because of its ability to quantify not only the states of conversion between land-use types, but also the relative rate of conversion (Subedi et al. 2013).

Few studies of LULC change provided a combined assessment of the driving forces and consequences of such variations, particularly in Africa (Reid et al. 2000). Recent research focused on sub-Saharan Africa, showing a decrease of land covered by the natural environment, mostly due to human activities such as population growth, economic development, and globalization (Mussa et a. 2017; Näschen et al. 2019). However, only a few studies tried to explicitly connect such changes with the loss of ecosystem services (Tolessa et al. 2017).

In this region, the dynamics of LULC intensities and rates are changing and highly associated with overexploitation of natural resources, while the process is governed by climate (long dry periods followed by heavy precipitation), soil characteristics (thin layer of topsoil, silty texture, or low organic matter content), vegetation (barren land), topography (steep-slope), and natural hazards (forest fire, landslides) (Nasir and Selvakumar, 2018; Leta et al. 2021b). During the last decades, the human pressure increased significantly, therefore the process has been accelerated considerably. In Ethiopia, LULC changes are persistent events where agricultural activities and settlements are dominant in the rural landscape (e.g., Alemu et al. 2015; Dibaba et al. 2020; Hailu et al. 2020). For example, Tadese et al. (2021) reported that the agricultural and settlement increased by around 17% and 3%, respectively, from 1987 to 2017 while agricultural land decreased by 78%.

Focusing on the Fincha River basin in Ethiopia, this research aims to: i) understand the historical LULC changes in the past three decades (1989–2019); ii) predict possible LULC patterns in the future three decades (2030-2050). The objectives of the paper will be tackled by combining satellite imagery (Landsat dataset) and modelling (LCM), using field evidence to support the study. The study area and the used methods will be described in Section 2, while the results are presented and discussed in Section 3.

2. Materials And Methods

2.1 Study Area

The Fincha watershed is located in Ethiopia, Oromiyaa regional state, Horroo Guduruu Wallaggaa, in the in Upper Blue Nile Basin (UBNB), between latitudes 9°9'53" N to 10°1'00" N and longitudes 37°00'25" E to 37°33'17" E, at around 300km from Addis Ababa (Figure 1).

Four main seasons are characterizing the region: Summer, from June to August, with heavy rainfalls; Autumn from September to November, called harvest season; Winter, from December to February, is the dry season with frost in the morning especially in January; Spring, from March to May, with occasional showers, is the hottest season. The annual rainfall of the study area ranges between 1367 and 1842 mm with the minimum rainfall occurring in the Northern lowlands and maximum rainfall greater than 1500mm rain in the Southern and Western highlands. From June to September is the main rainy season of the catchment, with an average of 1604 mm and the maximum rainfall between July to August.

Natural resources such as the Fincha, Amarti and Nashee lakes contribute to the national economy by generating hydroelectric power, but are also used for irrigating large fields devoted to sugar cane. The area is of interest for national and international hydro-politics due to its downstream connection to the Nile basin and the intense agriculture.

2.2 Dataset

The study was performed using freely available satellite imagery and a Digital Elevation Model (DEM). The latter, having a resolution of 30m and referring to 2019, was acquired from the GIS and Remote Sensing Department, Ministry of Water, Irrigation and Energy of Ethiopia.

Landsat-5 TM (L5, for the years 1989 and 2004) and Landsat-8 OLI-TIRS (L8, for the year 2019) data were downloaded from the United State Geological Survey (USGS) website (earthexplorer.usgs.gov). The images referred to January, when there is a clear sky corresponding to the dry season, and were atmospherically corrected via QGIS (qgis.org). To cover the whole watershed area, a composite of Landsat images from different paths/rows was created, assuring that the images refer to the same season (Table 1).

Table 1
Details of Landsat images.

Satellite	*Year*	*Acquisition date*	*Path/Row*	*Spatial Resolution*
Landsat 5 TM	1989	January 4	169/53, 169/54	30 m
		January 11	170/53	30 m
Landsat 5 TM		January 11	170/53	30 m
		January 15	169/53, 169/54	30 m
Landsat 8 OIL	2019	January 14	170/53	30 m
		January 23	169/53, 169/54	30 m

Field surveys have been conducted to assist the LULC classification of the satellite images. In addition, key informant interviews (KII) and focal group discussions were performed to obtain socio-economic support data, as this is paramount to understand how locals interact with the environment (Betru et al. 2019; Dibaba et al. 2020). KII were conducted with elders, as they have known the area for at least 30 years and had good knowledge on past LULC changes Focal group discussion was conducted with experts from zonal and district offices of Agriculture, Natural resources management, Environment and climatic change, Land use administration and local people's representatives. Ground truth data were collected using GPS and digital cameras to evaluate the current LULC.

2.3 Land use land cover classification of historical data

To map LULC, satellite images should be classified, assigning predefined LULC classes to some pixels. As pointed out by Jemberie et al. (2016), this phase could be affected by various factors such as classification methods, algorithms, collecting of training sites, and the quality (correctness) of the classification should be assessed via field evidence (Kindu et al. 2013; Abijith and Saravanan, 2021).

The study was performed classifying three reference years (1989, 2004, 2019), and accounting for six classes, as summarized in Table 2.

Table 2
Land use land cover classes and their description

LULC classes	*Description*
Waterbody	area completely covered by waters such as lakes, rivers and ponds
Built-up	area covered by urban and rural settlements, roads, industries, infrastructures
Agriculture	area covered by annual and perennial crops
Forest	area covered by evergreen forest
Shrub	area with trees that are not evergreen during the dry season
Grass/Swamp	area covered with grasses used for grazing, and sugarcane plantations

The maximum likelihood supervised classification method was applied via ArcGIS by creating training sites signature. Training sites for the L8 image of 2019 were defined using 100 ground truth points, while, for the two older L5 images, training signature sites were defined via unsupervised classification, ancillary data (Google Earth), KII information and literature data (Kenea et al. 2021). To improve image quality, quality assessments were used by taking a total of 50 ground truth points (20 agriculture, 5 waterbody, 5 built-up, 10 forest, 5 shrub, 5 grass/swamps).

To quantitatively assess the accuracy, statistical methods like overall accuracy and kappa value were applied. Based on this, random sampling data's were prepared to check the overall accuracy *OA* and to determine the Kappa coefficient *K*. Comparing the total corrected samples *TCS* and the total samples *TS*, *OA* provides an idea of how many sites are correctly classified (eq. 1), and spans from 0 (to corrected samples) to 1 (very accurate classification).

$$OA = \frac{TCS}{TS}$$

1

The Kappa coefficient *K* (eq. 2) is generated from a statistical test, and describes the accuracy of a classification compared to a random classification (Rwanga and Ndambuki, 2017; Aliani et al., 2019). Its value varies between 0 and 1, where 0 indicates a total accidental classification, while 1 indicates a very accurate classification. According to Gidey et al. (2017), good classifications have $K>0.8$, while bad classifications have $K<0.4$.

$$K = \frac{[TS * TCS - \sum (ColumnTotal * RowTotal)]}{TS^2 - \sum (ColumnTotal * RowTotal)}$$

2

where the matric columns indicate the correspondence between ground truth data and pixel location, while the matrix rows indicate to which class is the pixel assigned.

2.4 Prediction of future LULC and associated driving forces

To manage natural resources (biodiversity) influences, and to analyze and forecast spatial LULC changes, the Land Change Modeler (LCM) in TerrSet (formerly known as IDRISI) software was developed (Kumar et al. 2015; Aryaguna and Saputra 2020). LCM is an ArcGIS-integrated suite of tools for the assessment of future LULC changes, detecting gains and losses, net change, persistence and identification of transitions between LULC classes (Mishra et al. 2018). To map future LULC scenarios, LCM utilizes historical LULC maps and a series of driving forces (Table 3). The Markov chain

projection is performed by creating matrixes to estimate the transition probability and the area of each LULC class for future dates (Hasan et al. 2020; Khoshnood Motlagh et al. 2021).

Table 3
Driving variables considered in the LCM simulations.

Driving force	*Type*
Distance from disturbance	Dynamic
Distance from stream	Dynamic
Distance from urban	Dynamic
Distance from road	Dynamic
Evidence likelihood	Dynamic
Elevation	Static
Slope	Static

In this study, LCM was applied to forecast the future LULC in three scenarios (2030, 2040, 2050), via a few main steps: i) analysis of historical LULC maps (1989, 2004, 2019) and associated changes, ii) creation of transition probability matrixes, iii) model validation, iv) prediction of future LULC maps, accounted for possible driving forces.

To evaluate the capability of LCM in predicting future LULC, a predicted map of 2019 was created based on 1989 and 2004 LULC, and then compared with the actual 2019 map. To evaluate the quality of the 2019 predicted map against the 2019 reference map, the TerrSet validation module was used in TerrSet. Kappa indices such as kappa for no information (*Kno*), Kappa for Location (*Klocation*) and Kappa standards (*Kstandards*) are used to identify potential errors (Ibrahim et al 2016; Wang et al. 2018; Leta et al. 2021a). Kappa values vary between 0 and 1, with values >0.8 meaning an almost perfect agreement. In detail, *Kstandards* is an index of agreement that attempts to account for the expected agreement due to random spatial reallocation of the categories in the comparison map; *Kno* is identical to *Kstandards* if both the quantity and allocation of categories in the comparison map are selected randomly; *Klocation* represents the extent to which the maps agree in terms of location of each LULC category.

To corroborate the study outcomes, a series of statistics were considered (Wang et al. 2016): agreement due to chance (agreement chance), agreement due to quantity (agreement quantity), agreement due to the location at the grid cell level (agreement grid cell), disagreement due to the location at the grid cell level (disagree grid cell) and disagreement due to quantity (disagree quantity) were calculated to indicate how well the comparison map agrees with the reference map (Wang et al. 2016).

Driving forces are the factors that affect LULC changes at the local scale, and therefore they should be locally investigated and addressed (Eastman 2009; Khan et al. 2021). In simulating future LULC, LCM differentiates between static and dynamic variables, where the first are stable in time while the latter are temporally changing, and therefore recalculate every time-step (Table 3).

The Cramer's *V* Coefficient (*CVC*), sometimes also called Cramer's *V* strategies, was used to assess the correlations between the various driving variables. According to Eastman (2009), variables that have a Cramer's *V*>0.40 are good and

these drivers will have the greatest impact on the modification process and its spatial distribution (Gaur et al. 2020; Benavidez-Silva et al. 2021; Vu et al. 2021).

2.5 LULC detection

LULC changes were detected via a few parameters: magnitude of change *C*, rate of change *R* and change percentage *P*, via the following equations (Kafi et al. 2014; Leta et al. 2021a; Vivekananda et al. 2021).

$$C_i = L_i - B_i$$

3

$$R_i = \frac{L_i - B_i}{T}$$

4

$$P_i = \frac{L_i - B_i}{B_i} * 100$$

5

where *i* represents the LULC class, B_i and L_i are the areas [ha] with the earlies and latter LULC, respectively. The period between B_i and L_i is *T* [year], and determines the rate of change R_i. Positive values of P_i mean an increase of a specific LULC in the study period *T* ($L_i > B_i$, $R_i > 0$), while negative values a decrease ($L_i < B_i$, $R_i < 0$).

3. Results And Discussion

3.1 Historical LULC maps

Three reference years (1989, 2004, 2019) were considered to evaluate historical LULC, via a maximum likelihood supervised classification (Figure 2). As reported in Table 4, in 1989 most of the study area was covered by agriculture (33%), grass/swamps (24%), and shrub (22%), with only a very minor part occupied by built-up (0.3%). Similar LULC was also observed in 2014, with agriculture (34%), grass/swamp (24%) and shrub (18%) being the most dominant LULC classes, and just a small increase in the area covered by built-up (1%). In 2019, the class distribution remained more or less similar, with an increase in the built-up area (1.75%). In summary, in the past, agriculture was always the most dominant LULC class in the Fincha watershed, followed by grass/swamp and shrub.

Table 4
Details of LULC area of the Fincha watershed in the three reference years.

LULC type	*1989*		*2004*		*2019*	
	[ha]	*[%]*	*[ha]*	*[%]*	*[ha]*	*[%]*
Waterbody	15744.08	5.24	19928.15	6.63	20860.55	6.94
Grass/Swamp	73371.25	24.42	73423.56	24.43	73570.49	24.48
Built-up	1252.00	0.42	2945.40	0.98	5007.75	1.67
Agriculture	96966.71	32.27	103033.14	34.29	115446.96	38.42
Forest	48373.16	16.10	46569.29	15.50	29213.93	9.72
Shrub	64790.11	21.56	54597.77	18.17	56397.63	18.77
Total	300497.31	100.00	300497.31	100.00	300497.31	100.00

The results reported in Figure 2 are in agreement with Dibaba et al. (2016), who pointed out that the Fincha watershed is characterized by an expansion of agriculture and built-up LULC, resulting in a decline of natural vegetation.

3.2 Accuracy assessment for historical LULC

The overall accuracies *OA* and Kappa values *K* were 82.80%, 85.57%, 89.82% and 80.51%, 82.54% and 87.84%, respectively, for the three reference years (Table 5 and supplementary Tables S1, S2, S3). These results indicate that the accuracy of the classifications improved from 1989 to 2019, also thanks to the higher quality of the satellite data used.

Table 5
LULC classification accuracy for 1989, 2004 and 2019.

Year	*LULC class*	*Producer Accuracy*	*User Accuracy*	*OA [%]*	*K [%]*
1989	Waterbody	92.86	89.66	82.80	80.51
	Grass/Swamp	76.78	86.00		
	Built-up	84.61	84.62		
	Agriculture	82.69	74.14		
	Forest	85.71	87.80		
	Shrub	80.43	80.43		
2004	Waterbody	97.06	91.67	85.57	82.54
	Grass/Swamp	75.14	84.13		
	Built-up	83.87	86.67		
	Agriculture	88.41	81.33		
	Forest	89.80	93.62		
	Shrub	84.62	81.48		
2019	Waterbody	94.44	85.00	89.82	87.84
	Grass/Swamp	86.30	87.50		
	Built-up	97.14	91.89		
	Agriculture	90.45	95.00		
	Forest	89.29	92.59		
	Shrub	86.67	85.25		

The accuracy of a map could be different for users and map developers. The user's accuracy indicates how often a specified class on the map is present on the ground, while the producer's (mapmaker) accuracy shows how frequently are real futures on the ground appropriately shown on the classified map or the probability that a certain land cover is classified according to field evidence.

Hailu et al. (2020) defined the Kappa statistics <40%, 40%-75% and >75% as poor, good and excellent, respectively. Using this approach, from Table 5 one can notice that the statistics of the Fincha watershed were excellent, meaning a very good agreement between the classification maps and the reference information.

3.3 Historical LULC changes and transition probability matrix

Comparing the three reference years, it is possible to observe a considerable reduction in the area covered by forest and shrubs during the observation period (Table 6). In detail, yearly, around 639 ha of forest and 280 ha of shrub were cleared in favour of other LULC classes. As anticipated, human pressure contributed to changing the environment, as recognizable by the increase in areas covered by agricultural fields, built-up, grass/swamp and waterbodies, which yearly gained around 616 ha, 125 ha, 7 ha and 171 ha, respectively. Waterbodies increased significantly during the last 30 years, mainly because of human intervention. In fact, in 1989, the Amerti reservoir, one of the reservoirs located in the Fincha watershed, was not fully filled, while it was filled in 2014. In 2019, another dam was constructed over the Nashe

River (Leta et al. 2021a). The study pointed out small changes in terms of grass/swamps, at least in terms of net variation. In fact, as visible from Figure 3 and Table 6, the majority of the Fincha watershed was affected by variations in LULC that include this class.

Table 6
Historical LULC changes in the Fincha watershed.

	1989-2004			*2004-2019*			*1989-2019*		
LULC Class	*area [ha]*	*area [%]*	*change [ha/year]*	*area [ha]*	*area [%]*	*change [ha/year]*	*area [ha]*	*area [%]*	*change [ha/year]*
Agriculture	6,067.5	6.3	404.5	12,412.7	12.1	827.5	18,480.3	19.06	616.0
Built-up	1,693.4	135.3	112.9	2,062.3	70.0	137.5	3,755.8	300.0	125.2
Forest	-1,803.9	-3.7	-120.3	-17,355.4	-37.3	-1157.0	-19,159.2	-39.6	-638.6
Grass/Swamps	52.3	0.1	3.5	146.9	0.2	9.8	199.2	0.3	6.6
Shrub	-10,192.3	-15.7	-679.5	1,799.9	3.3	120.0	-8,392.5	-13.0	-279.8
Waterbody	4,183.0	26.6	278.9	933.4	4.7	62.2	5,116.3	32.5	170.5

The results presented here are in line with the existing literature on LULC in the Fincha watershed (e.g., Dibaba et al. 2020; Leta et al. 2021b). All the authors agreed that the shifting from natural LULC towards more anthropized environments could threaten biodiversity and decrease the total values of ecosystem services (Tolessa et al. 2021)

The probability transitional matrix is the transfer direction of Land use land cover types from one category to other categories in the given year (Han et al. 2015). The nature change can be distinguished from the Markov transitional matrices for historical LULCC over the period between (1989-2004 and 2004-2019). The nature of change can be distinguished from the trend as depicted from the Markov transition matrices over the period between 1989 and 2019. The diagonal values represent the probability that each land cover class remains persistent (constant) from earlier to later years. The other values represent a given land cover land class undertakes transition to another land cover land class.

Between 1989 and 2004, the highest and the lowest persistent LULC classes were waterbody and grass/swamps, characterized by a percentage of stability of 91% and 42%, respectively. During the period 2004-2019, the most and the less stable LULC class categories were waterbody and grass/swamp, which accounted for around 80% and 31%, respectively. Over the entire temporal horizon observed (1989 to 2019), a large part of the forest was converted to agriculture and grass/swamps (see Tables S4, S5 and S6 for the detailed LULC transition matrixes).

According to information obtained during field investigations (KII and field evidence), waterbodies increased after the newly constructed Nashe Dam. During the construction of the reservoir, many farmers along and downstream of the Nashe stream had been displaced to other agricultural places or towns. The abandonment of fields and the need for resettling in other areas caused a decrease in forest and an increase in built-up areas. In addition, not well-planned and long-term urban development and agricultural management strategies contributing to negatively affecting natural resources, causing its significant decline in the last decades (Figure 3).

3.4 Model validation

The LULC map of 2019, predicted from the 1989 and 2004 data, has been validated with the classified LULC map of the very same year (Table 7), showing that the LCM model can effectively forecast LULC changes.

Table 7
LULC classes in 2019: projected vs classified values.

	Projected LULC		***Classified LULC***	
LULC Class	*Area [ha]*	*Percentage [%]*	*Area [ha]*	*Percentage [%]*
Waterbody	19942.55	6.64	20861.54	6.94
Grass/swamp	76883.19	25.58	73570.84	24.48
Built-up	3007.232	1.00	5007.76	1.67
Agriculture	108578.3	36.13	115449.74	38.42
Forest	48717.03	16.21	29214.18	9.72
Shrub	43377.06	14.43	56401.33	18.77
Total	300505.4	100.00	300505.40	100.00

The capability of LCM in predicting the 2019 LULC was assessed via *K*-indexes and other statistics in TerrSet (Table 8). All the values of k-indexes (>80%) indicate good agreement between the projected and the actual LULC map (Leta et al. 2021a). The Disagree Quantity (0.0742) is greater than the Disagree Gridcell (0.0268), indicating that the model has a higher ability to predict the LULC in location (spatial) than in quantity for the Fincha watershed. To corroborate the results presented here and to reduce the uncertainties, additional data should be included in the study, mostly deriving from laborious and expensive field investigations.

Table 8
Statistics of using the Multi-layer Perceptron Markov Chain (MLP_MC) model for predicting LULC in 2019.

Statistics	***Value***
Kno	0.8743
Klocation	0.8864
Kstandards	0.8285
Agreement Chance	0.1667
Agreement Quantity	0.3252
Agreement Gridcell	0.4071
Disagreement Gridcell	0.0268
Disagreement Quantity	0.0742

3.5 Future LULC

To forecast future LULC changes, it is needed to account for the most important driving variables (Table 9). As visible, all variables but the slope should be included in LCM.

Table 9
Cramer's *V* value of driving variables

Driving force	*Cramer's V value*
Distance from disturbance	0.2782
Distance from stream	0.3240
Distance from urban	0.1548
Distance from road	0.2736
Evidence likelihood	0.4212
Elevation	0.2949
Slope	0.0101

The LULC maps for 2030, 2040 and 2050 were created via LCM, using the historical maps as a basis (Figure 4). As observed in the past, also for the future an increase in areas covered by agriculture, built-up, grass/swamp and waterbody is forecasted, while a drastic decrease in forest and shrub should be expected, with a slower rate of deforestation in the decade 2040-2050 (Figure 5 and Table 10). Since both forest and shrub will continuously decrease in the future, a major effort in promoting protection measures to keep natural resources and biodiversity is advisable.

Table 10
Future LULC changes in the Fincha watershed.

	2019-2030		*2030-2040*		*2040-2050*		*2019-2050*	
LULCC Class	*[ha]*	*[%]*	*[ha]*	*[%]*	*[ha]*	*[%]*	*[ha]*	*[%]*
Agriculture	7722.2	6.7	2795.1	2.3	1619	1.3	12136.3	10.5
Built-up	358.8	7.2	420.7	7.8	204.5	3.5	984	19.6
Forest	-13585.1	-46.5	-4374.9	-28.0	-1808.4	-16.1	-19768.4	-67.7
Grass/swamp	12589	17.1	1672.5	1.9	-235.5	-0.3	14026	19.1
Shrub	-9287.6	-16.5	-1309.8	-2.8	-392.8	-0.9	-10990.2	-19.5
Waterbody	2204.5	10.6	796.3	3.5	613.1	2.6	3613.9	17.3

In terms of transition probability (Tables S7, S8, S9), areas covered by forest and shrubs are more prone to be converted into agricultural land, while built-up areas should be expected on the actual grass/swamp zones. This indicates that, for the future, agriculture and built-up zones will expand at a high rate since the other LULC classes will be converted to them. Reversely, forests and shrubs will decline at a significant rate.

The LCM results point out that, in the incoming decades, significant changes in LULC should be expected, mostly because of an ever-increasing pressure of humans in need of more land for settlements and cropland. Indeed, the local

population is growing, and more natural resources are needed to satisfy their request for food, energy and construction material (Leta et al. 2021a; Kenea et al. 2021). Besides direct consequences on the environment, the ongoing deforestation in the Fincha basin is also causing an intensification of soil erosion, triggering sediment siltation in the various reservoirs located in the region, eventually leading to a decrease in reservoir efficiency in terms of water availability and hydropower production.

4. Conclusions

The present study investigated the historical LULC (years 1989, 204, 219) in the Ethiopian Fincha watershed via a combination of satellite imagery and field support data. Based on such analysis, the Land Change Modeller was applied to forecast LULC in the next three decades (years 2030, 2040, 2050). The 2019 LULC was also used for validating the LCM approach, comparing the forecasted situation with the actual one, indicating that the multi-layer Perceptron (MLP) neural network of Markov-Chain (MC) has enough capability to predict future LULC.

Over the last thirty years, the forest covering the Fincha watershed was mostly converted to agricultural and Grass/swamp areas. An increase in areas covered by waterbody and built-up was also observable, mainly connected with increasing human pressure and the construction of new hydropower reservoirs.

For the future, a similar trend is more than probable. Indeed, if management strategies will not change towards more sustainable ones, an even more significant decrease of the forest should be expected, in favour of new settlement areas and cropland. This change could help locals in sustaining their livelihood in the short term, but, in the medium/long term, the reduction of areas covered by forest will contribute to decreasing biodiversity and ecosystems services, as well as in fostering soil erosion, with detrimental consequences such as reservoir siltation.

Declarations

Author Contributions

Conceptualization, M.S.R. and M.N.; writing-original draft preparation, M.S.R. and M.N.; literature review, M.S.R. and M.N..; supervision, M.N.; project administration, M.N.; funding acquisition, M.N.

Funding

This research was funded by NCN National Science Centre Poland–call PRELUDIUM BIS-1, Grant Number 2019/35/O/ST10/00167. Project website: https://sites.google.com/view/lulc-fincha/home.

Competing interests

The authors declare no competing interests.

References

Abijith, D., & Saravanan, S. (2021). Assessment of land use and land cover change detection and prediction using remote sensing and CA Markov in the northern coastal districts of Tamil Nadu, India. Environmental Science and Pollution Research, 1-13.

Al-sharif, A. A., & Pradhan, B. (2014). Monitoring and predicting land use change in Tripoli Metropolitan City using an integrated Markov chain and cellular automata models in GIS. Arabian Journal of Geosciences, 7(10), 4291-4301.

Alam, A., Bhat, M. S., & Maheen, M. (2020). Using Landsat satellite data for assessing the land use and land cover change in Kashmir valley. GeoJournal, 85(6), 1529-1543.

Alemu, B., Garedew, E., Eshetu, Z., & Kassa, H. (2015). Land use and land cover changes and associated driving forces in north western lowlands of Ethiopia. Int. Research Journal of Agricultural Science and Soil Science, 5(1), 28-44.

Aliani, H., Malmir, M., Sourodi, M., & Kafaky, S. B. (2019). Change detection and prediction of urban land use changes by CA–Markov model (case study: Talesh County). Environmental Earth Sciences, 78(17), 1-12.

Aryaguna, P. A., & Saputra, A. N. (2020). Land change modeler for predicting land cover change in Banjarmasin City, South Borneo (2014-2022). In IOP Conference Series: Earth and Environmental Science, 500(1), 012002.

Benavidez-Silva, C., Jensen, M., & Pliscoff, P. (2021). Future Scenarios for Land Use in Chile: Identifying Drivers of Change and Impacts over Protected Area System. Land, 10(4), 408.

Betru, T., Tolera, M., Sahle, K., & Kassa, H. (2019). Trends and drivers of land use/land cover change in Western Ethiopia. Applied Geography, 104, 83-93.

Dibaba, W. T., Demissie, T. A., & Miegel, K. (2020). Drivers and implications of land use/land cover dynamics in Finchaa catchment, northwestern Ethiopia. Land, 9(4), 113.

Dwivedi, R. S., Sreenivas, K., & Ramana, K. V. (2005). Cover: Land-use/land-cover change analysis in part of Ethiopia using Landsat Thematic Mapper data. International Journal of Remote Sensing, 26(7), 1285-1287.

Eastman, J. R. (2009). IDRISI Taiga guide to GIS and image processing. Clark Labs Clark University, Worcester, MA., USA

Etemadi, H., Smoak, J. M., & Karami, J. (2018). Land use change assessment in coastal mangrove forests of Iran utilizing satellite imagery and CA–Markov algorithms to monitor and predict future change. Environmental Earth Sciences, 77(5), 1-13.

Fan, F., Wang, Y., & Wang, Z. (2008). Temporal and spatial change detecting (1998–2003) and predicting of land use and land cover in Core corridor of Pearl River Delta (China) by using TM and ETM+ images. Environmental Monitoring and Assessment, 137(1), 127-147.

Gaur, S., Mittal, A., Bandyopadhyay, A., Holman, I., & Singh, R. (2020). Spatio-temporal analysis of land use and land cover change: a systematic model inter-comparison driven by integrated modelling techniques. Int. Journal of Remote Sensing, 41(23), 9229-9255.

Gidey, E., Dikinya, O., Sebego, R., Segosebe, E., & Zenebe, A. (2017). Modeling the Spatio-temporal dynamics and evolution of land use and land cover (1984–2015) using remote sensing and GIS in Raya, Northern Ethiopia. Modeling Earth Systems and Environment, 3(4), 1285-1301.

Hailu, A., Mammo, S., & Kidane, M. (2020). Dynamics of land use, land cover change trend and its drivers in Jimma Geneti District, Western Ethiopia. Land Use Policy, 99, 105011.

Han, H., Yang, C., & Song, J. (2015). Scenario simulation and the prediction of land use and land cover change in Beijing, China. Sustainability, 7(4), 4260-4279.

Hasan, S., Shi, W., Zhu, X., Abbas, S., & Khan, H. U. A. (2020). Future simulation of land use changes in rapidly urbanizing South China based on land change modeler and remote sensing data. Sustainability, 12(11), 4350.

Ibrahim M. M., Duker, A., Conrad, C., Thiel, M., & Shaba Ahmad, H. (2016). Analysis of settlement expansion and urban growth modelling using geoinformation for assessing potential impacts of urbanization on climate in Abuja City, Nigeria. Remote Sensing, 8(3), 220.

Jemberie, M., Gebrie, T., & Gebremariam, B. (2016). Evaluation of land use land cover change on stream flow: A case study of Dedissa Sub Basin, Abay Basin, South Western Ethiopia. International Journal of Innovations in Engineering Research and Technology, 3, 2394–3696.

Kafi, K. M., Shafri, H. Z. M., & Shariff, A. B. M. (2014). An analysis of LULC change detection using remotely sensed data; A Case study of Bauchi City. In IOP conference series: Earth and Environmental Science, 20(1), 012056.

Kenea, U., Adeba, D., Regasa, M. S., & Nones, M. (2021). Hydrological Responses to Land Use Land Cover Changes in the Fincha'a Watershed, Ethiopia. Land, 10(9), 916.

Khan, T. U., Mannan, A., Hacker, C. E., Ahmad, S., Amir Siddique, M., Khan, B. U., ... & Luan, X. (2021). Use of GIS and Remote Sensing Data to Understand the Impacts of Land Use/Land Cover Changes (LULCC) on Snow Leopard (Panthera uncia) Habitat in Pakistan. Sustainability, 13(7), 3590.

Khoshnood Motlagh, S., Sadoddin, A., Haghnegahdar, A., Razavi, S., Salmanmahiny, A., & Ghorbani, K. (2021). Analysis and prediction of land cover changes using the land change modeler (LCM) in a semiarid river basin, Iran. Land Degradation & Development, 32(10), 3092-3105.

Kindu, M., Schneider, T., Teketay, D., & Knoke, T. (2013). Land use/land cover change analysis using object-based classification approach in Munessa-Shashemene landscape of the Ethiopian highlands. Remote Sensing, 5(5), 2411-2435.

Kumar, K. S., Bhaskar, P. U., & Padmakumari, K. (2015). Application of land change modeler for prediction of future land use land cover: a case study of Vijayawada City. International Journal of Advanced Technology in Engineering and Science, 3(01), 773-783.

Lambin, E. F., Rounsevell, M. D., & Geist, H. J. (2000). Are agricultural land-use models able to predict changes in land-use intensity?. Agriculture, Ecosystems & Environment, 82(1-3), 321-331.

Leta, M. K., Demissie, T. A., & Tränckner, J. (2021a). Hydrological Responses of Watershed to Historical and Future Land Use Land Cover Change Dynamics of Nashe Watershed, Ethiopia. Water, 13(17), 2372.

Leta, M. K., Demissie, T. A., & Tränckner, J. (2021b). Modeling and Prediction of Land Use Land Cover Change Dynamics Based on Land Change Modeler (LCM) in Nashe Watershed, Upper Blue Nile Basin, Ethiopia. Sustainability, 13(7), 3740.

Mishra, V. N., Rai, P. K., Prasad, R., Punia, M., & Nistor, M. M. (2018). Prediction of spatio-temporal land use/land cover dynamics in rapidly developing Varanasi district of Uttar Pradesh, India, using geospatial approach: a comparison of hybrid models. Applied Geomatics, 10(3), 257-276.

Mussa, M., Teka, H., & Mesfin, Y. (2017). Land use/cover change analysis and local community perception towards land cover change in the lowland of Bale rangelands, Southeast Ethiopia. International Journal of Biodiversity and Conservation, 9(12), 363-372.

Näschen, K., Diekkrüger, B., Evers, M., Höllermann, B., Steinbach, S., & Thonfeld, F. (2019). The impact of land use/land cover change (LULCC) on water resources in a tropical catchment in Tanzania under different climate change scenarios. Sustainability, 11(24), 7083.

Nasir, N., & Selvakumar, R. (2018). Influence of land use changes on spatial erosion pattern, a time series analysis using RUSLE and GIS: the cases of Ambuliyar sub-basin, India. Acta Geophysica, 66(5), 1121-1130.

Rahman, M. T. U., Tabassum, F., Rasheduzzaman, M., Saba, H., Sarkar, L., Ferdous, J., ... & Islam, A. Z. (2017). Temporal dynamics of land use/land cover change and its prediction using CA-ANN model for southwestern coastal Bangladesh. Environmental Monitoring and Assessment, 189(11), 1-18.

Regasa, M. S., Nones, M., & Adeba, D. (2021). A Review on Land Use and Land Cover Change in Ethiopian Basins. Land, 10(6), 585.

Reid, R. S., Kruska, R. L., Muthui, N., Taye, A., Wotton, S., Wilson, C. J., & Mulatu, W. (2000). Land-use and land-cover dynamics in response to changes in climatic, biological and socio-political forces: the case of southwestern Ethiopia. Landscape Ecology, 15(4), 339-355.

Rwanga, S. S., & Ndambuki, J. M. (2017). Accuracy assessment of land use/land cover classification using remote sensing and GIS. International Journal of Geosciences, 8(04), 611.

Subedi, P., Subedi, K., & Thapa, B. (2013). Application of a hybrid cellular automaton–Markov (CA-Markov) model in land-use change prediction: a case study of Saddle Creek Drainage Basin, Florida. Applied Ecology and Environmental Sciences, 1(6), 126-132.

Tadese, S., Soromessa, T., & Bekele, T. (2021). Analysis of the current and future prediction of land use/land cover Change using remote sensing and the CA-markov model in majang forest biosphere reserves of Gambella, southwestern Ethiopia. The Scientific World Journal, 2021.

Tolessa, T., Senbeta, F., & Kidane, M. (2017). The impact of land use/land cover change on ecosystem services in the central highlands of Ethiopia. Ecosystem Services, 23, 47-54.

Tolessa, T., Kidane, M., & Bezie, A. (2021). Assessment of the linkages between ecosystem service provision and land use/land cover change in Fincha watershed, North-Western Ethiopia. Heliyon, 7(7), e07673.

Vivekananda, G. N., Swathi, R., & Sujith, A. V. L. N. (2021). Multi-temporal image analysis for LULC classification and change detection. European Journal of Remote Sensing, 54(2), 189-199.

Vu, T. T., & Shen, Y. (2021). Land-Use and Land-Cover Changes in Dong Trieu District, Vietnam, during Past Two Decades and Their Driving Forces. Land, 10(8), 798.

Wang, W., Zhang, C., Allen, J. M., Li, W., Boyer, M. A., Segerson, K., & Silander, J. A. (2016). Analysis and prediction of land use changes related to invasive species and major driving forces in the state of Connecticut. Land, 5(3), 25.

Wang, J., & Maduako, I. N. (2018). Spatio-temporal urban growth dynamics of Lagos Metropolitan Region of Nigeria based on Hybrid methods for LULC modeling and prediction. European Journal of Remote Sensing, 51(1), 251-265.

Figures

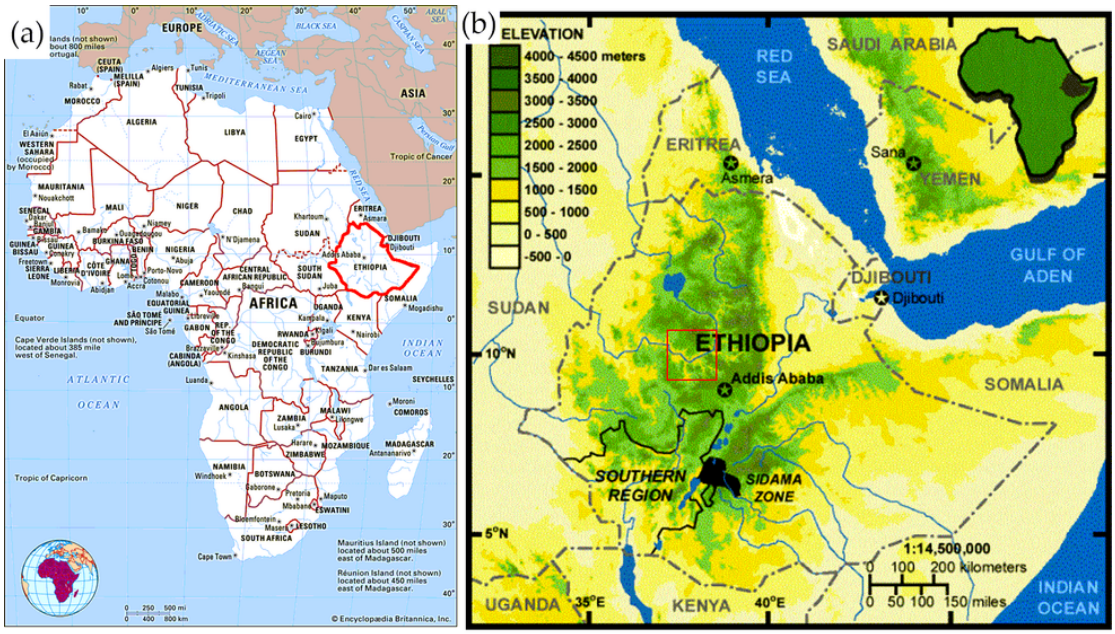

Figure 1

(a) Map of Africa; (b) map of Ethiopia with ground elevation; (c) Digital Elevation model (DEM) of the Fincha watershed. Adapted from Kenea et al. (2021).

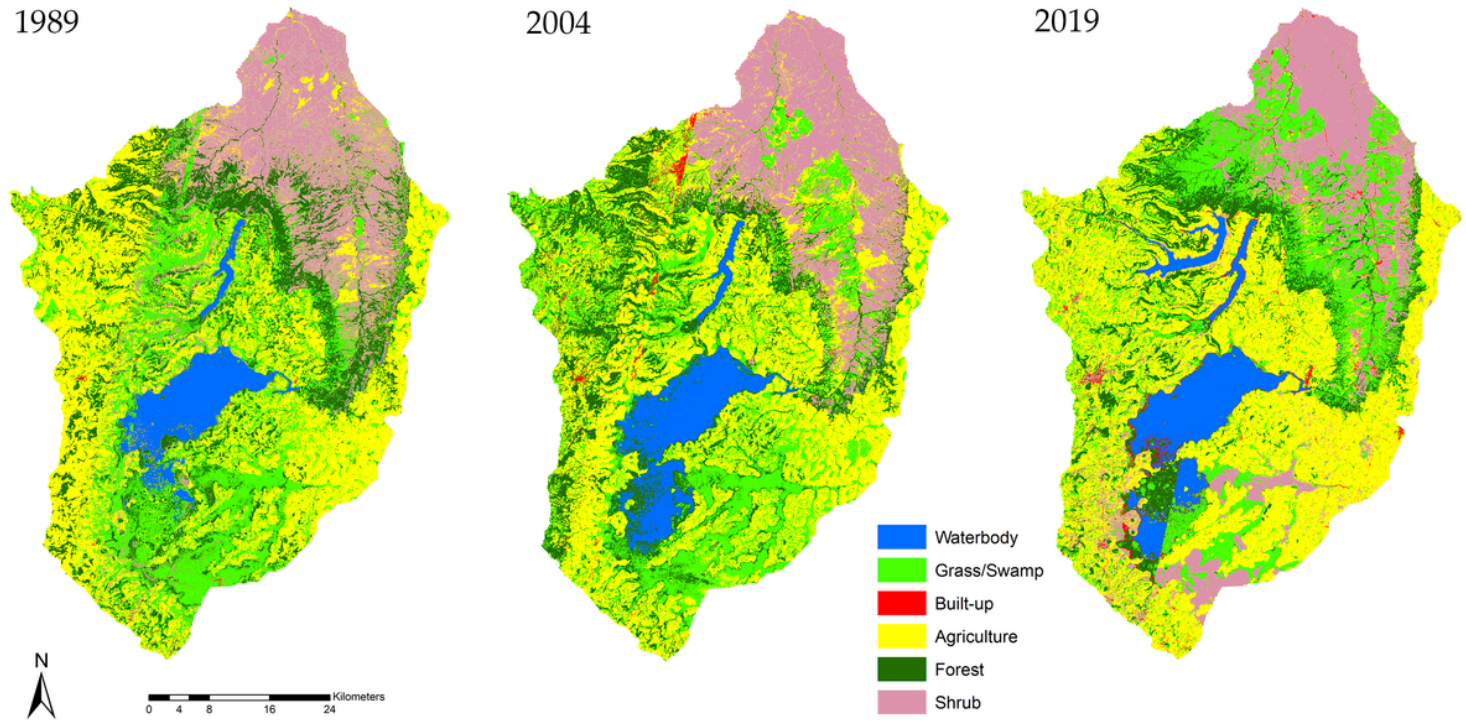

Figure 2

LULC maps of the Fincha watershed in the three reference years.

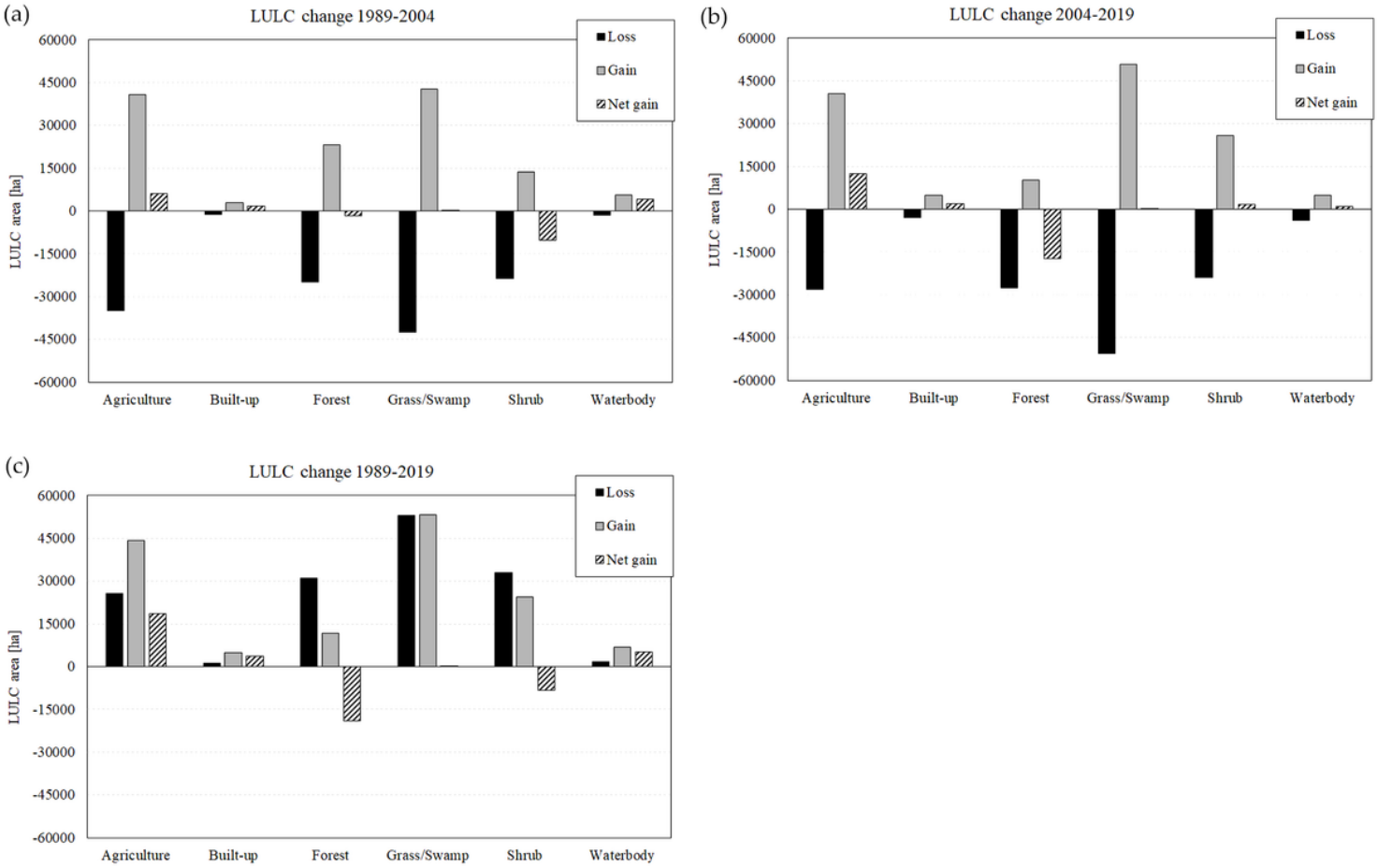

Figure 3

LULC changes during the observed period: (a) from 1989 to 2004, (b) from 2004 to 2019, (c) from 1989 to 2019.

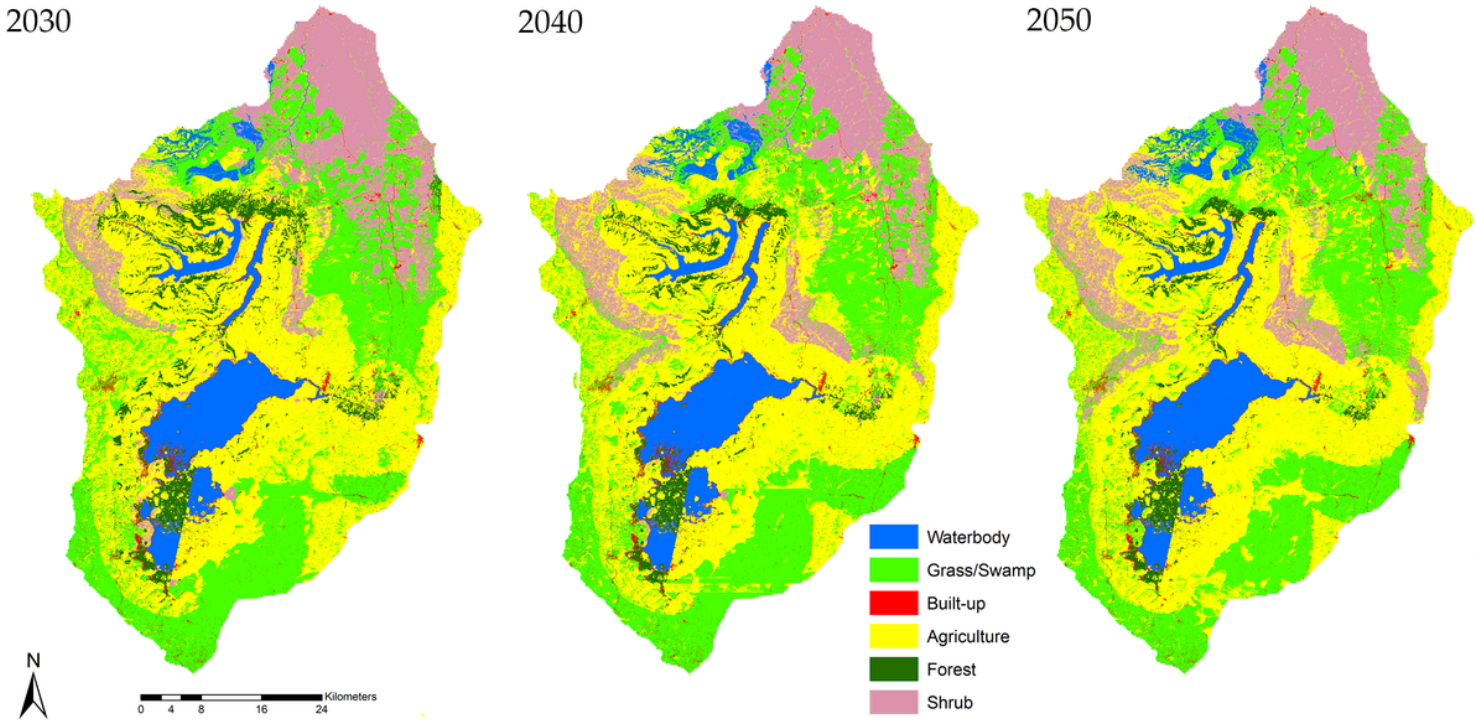

Figure 4

Predicted LULC of the Fincha watershed for the next three decades.

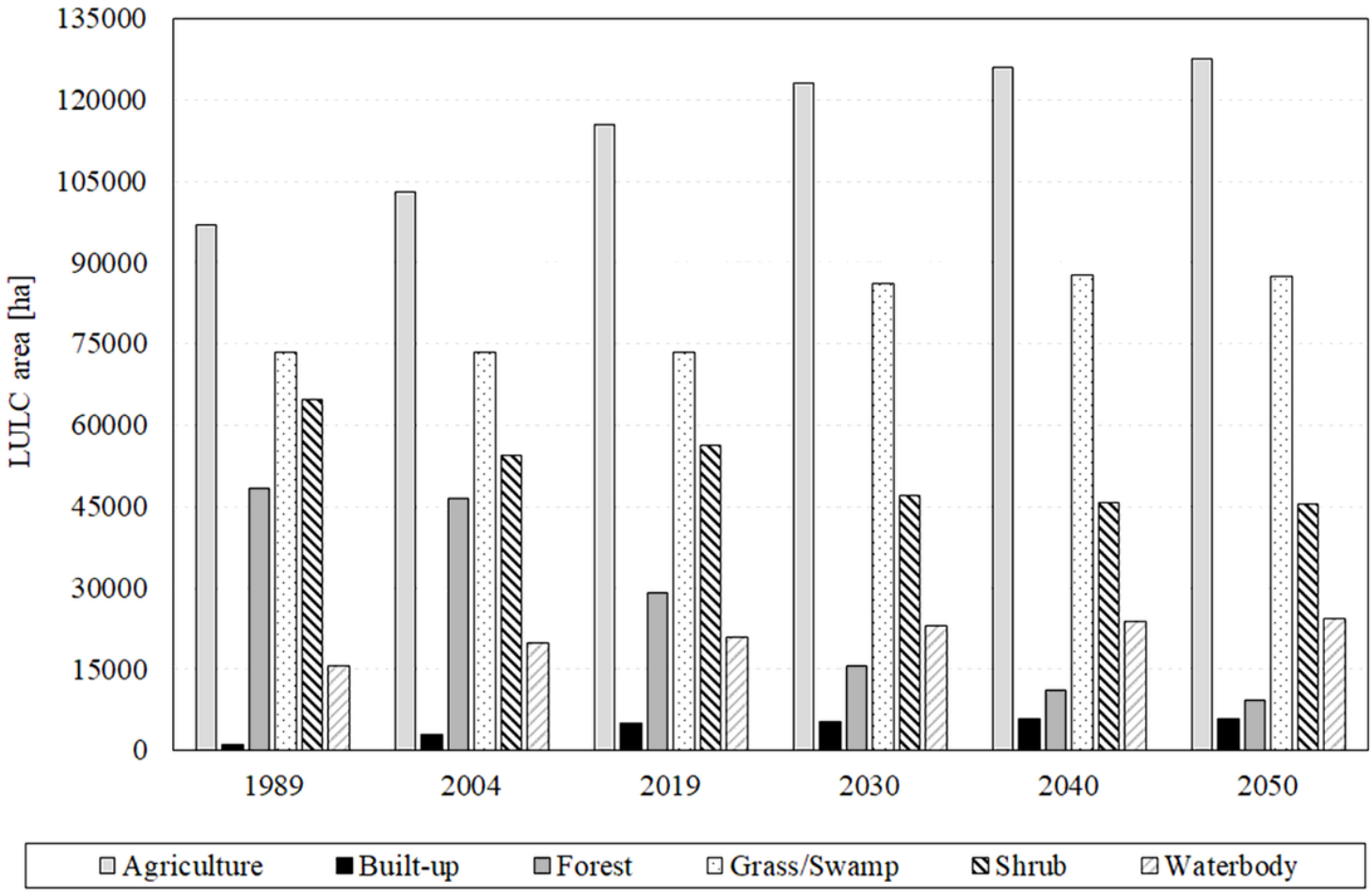

Figure 5

Observed (1989, 2004, 2019) and simulated (2030, 2040, 2050) LULC in the Fincha watershed.

Supplementary Files

This is a list of supplementary files associated with this preprint. Click to download.

- supplmaterial.docx